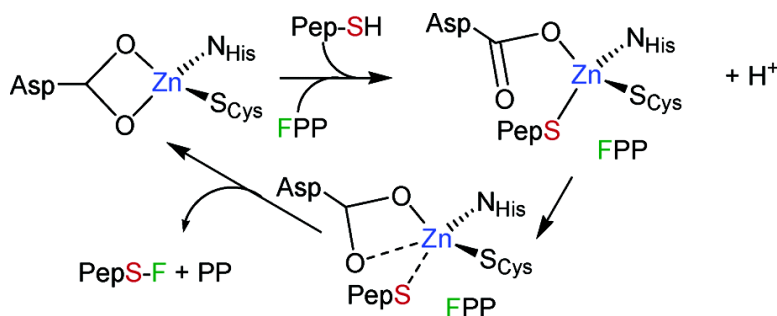Article

Structural Characterization of the Zinc Site in Protein Farnesyltransferase

Daniel A. Tobin, Jennifer S. Pickett, Heather L. Hartman, Carol A. Fierke, and James E. Penner-Hahn

More About This Article

Additional resources and features associated with this article are available within the HTML version:

- Supporting Information
- Links to the 11 articles that cite this article, as of the time of this article download
- Access to high resolution figures
- Links to articles and content related to this article
- Copyright permission to reproduce figures and/or text from this article

View the Full Text HTML

Structural Characterization of the Zinc Site in Protein Farnesyltransferase

Daniel A. Tobin,[†] Jennifer S. Pickett,[†] Heather L. Hartman,[†] Carol A. Fierke,*,[†] and James E. Penner-Hahn*,[†,‡]

Contribution from the Department of Chemistry and the Biophysics Research Division, The University of Michigan, Ann Arbor, Michigan 48109-1055

Received May 2, 2003; E-mail: fierke@umich.edu; jeph@umich.edu

Abstract: X-ray absorption spectroscopy has been used to determine the structure of the Zn site in protein farnesyltransferase. Extended X-ray absorption fine structure (EXAFS) data are consistent with a Zn site that is ligated to three low-Z (oxygen or nitrogen) ligands and one cysteine sulfur, as predicted from the crystal structures that are available for farnesyltransferase. However, in contrast with the crystallographic results the EXAFS data do *not* show evidence for significant distortions in the Zn−ligand distances. The average Zn−(N/O) and Zn−S distances are 2.04 and 2.31 Å, respectively. Addition of a farnesyl diphosphate analogue causes no detectable change in the structure of the Zn site. However, addition of peptide substrate causes a change in ligation from $ZnS(N/O)_3$ to $ZnS_2(N/O)_2$, consistent with ligation of the C-terminal cysteine to the Zn. There is no significant change in Zn−ligand distances when a substrate binds, demonstrating that the Zn remains four-coordinate. Addition of both peptide and farnesyl diphosphate to give the product complex causes the Zn to return to $ZnS(N/O)_3$ ligation, indicating that the product thioether is not tightly coordinated to the Zn. These spectroscopic experiments provide insight into the catalytic mechanism of FTase.

Farnesylation is a critical post-translational modification in mammalian cells. The addition of a farnesyl group (a 15-carbon isoprenoid polyunsaturated hydrocarbon chain) to a protein enhances the association with a lipid bilayer and/or facilitates protein−protein interactions. Farnesylated proteins such as the Ras family and G proteins are involved in signal transduction, and their activity has been implicated in both cancer and tumor growth. Farnesyltransferase (FTase) catalyzes the transfer of the farnesyl group of farnesyl diphosphate (FPP) to the cysteine in a C-terminal CaaX sequence of the target protein. FTase is an α/β heterodimer, with one required zinc per β subunit.[1−3]

The zinc in FTase is bound by Asp 297, His 362, Cys 299, and a water molecule when the enzyme is in its resting state, as demonstrated by the X-ray crystal structure.[2] The kinetic mechanism of FTase is functionally ordered with FPP binding first to a groove adjacent to the zinc site, followed by binding of the CaaX sequence of the target protein to form the ternary complex.[4] Crystallography and Co^{2+} UV−visible spectroscopy show that the cysteine thiolate of the target protein displaces the water and coordinates to the zinc.[1,5−7] FTase then catalyzes transfer of C1 of the farnesyl moiety to the zinc-bound thiolate

of the target protein cysteine with concomitant cleavage of the diphosphate group from FPP. FTase has been proposed to catalyze farnesylation through a transition state with dissociative character.[8,9] The transition state is proposed to have significant C1−O bond cleavage and modest C1−S bond formation so that C1 develops a partial positive charge. The coordination of the peptide sulfur to zinc in the ternary complex lowers the cysteine pK_a so the sulfur is present as a reactive thiolate at physiological pH.[10] Withdrawing electrons from the thiolate by replacement of zinc with thiophilic cadmium reduces the rate of product formation, signifying the value of the metal-bound thiolate to the reaction.[9]

FTase is one among a growing number of zinc-dependent alkyl transferase enzymes. The common feature of these enzymes is the zinc-promoted transfer of an alkyl group to a thiol substrate. The first example of this class of protein was the DNA demethylation protein Ada, where the "substrate" thiolate is an endogenous cysteine. To date this group includes cobalamine-dependent (MetH) and cobalamine-independent (MetE) methionine synthase,[11] protein farnesyltransferase (FTase),

† Department of Chemistry.
‡ Biophysics Research Division.

(1) Huang, C.-C.; Casey, P. J.; Fierke, C. A. *J. Biol. Chem.* **1997**, *272*, 20−23.
(2) Park, H.-W.; Boduluri, S. R.; Moomaw, J. F.; Casey, P. J.; Beese, L. S. *Science* **1997**, *275*, 1800−1804.
(3) Reiss, Y.; Brown, M. S.; Goldstein, J. L. *J. Biol. Chem.* **1992**, *267*, 6403−6408.
(4) Furfine, E. S.; Leban, J. J.; Landavazo, A.; Moomaw, J. F.; Casey, P. J. *Biochemistry* **1995**, *34*, 6857−6862.
(5) Long, S. B.; Casey, P. J.; Beese, L. S. *Structure* **2000**, *8*, 209−222.

(6) Strickland, C. L.; Windsor, W. T.; Syto, R.; Wang, L.; Bond, R.; Wu, Z.; Schwartz, J.; Le, H. V.; Beese, L. S.; Weber, P. C. *Biochemistry* **1998**, *37*, 16601−16611.
(7) Long, S. B.; Hancock, P. J.; Kral, A. M.; Hellinga, H. W.; Beese, L. S. *Proc. Natl. Acad. Sci. U.S.A.* **2001**, *98*, 12948−12953.
(8) Dolence, J. M.; Poulter, C. D. *Proc. Natl. Acad. Sci. U.S.A.* **1995**, *92*, 5008−5011.
(9) Huang, C. C.; Hightower, K. E.; Fierke, C. A. *Biochemistry* **2000**, *39*, 2593−2602.
(10) Hightower, K. E.; Huang, C. C.; Casey, P. J.; Fierke, C. A. *Biochemistry* **1998**, *37*, 15555−15562.
(11) Peariso, K.; Zhou, Z. H.; Smith, A. E.; Matthews, R. G.; Penner-Hahn, J. E. *Biochemistry* **2001**, *40*, 987−993.

and the related enzymes protein geranylgeranyltransferase types I and II,[12,13] betaine homocysteine methyltransferase (BHMT),[14] Ada protein,[15] epoxyalkane:CoM transferase, methylcobamide: coenzyme M methyl transferase MT2-A,[16] and its isozyme MT2-M.[16] In all cases, the substrate thiolate (the site of alkylation) appears to coordinate directly to the zinc. In addition to the substrate thiolate, the Zn is coordinated to one (FTase and GGTase), two (MetE, MT2-A), or three (Ada, BHMT, MetH) cysteine ligands. The protein prenyltransferase family (FTase and GGTase) is the only example within the class in which there is only a single nonsubstrate sulfur bound to the zinc. The role of the zinc ion in the catalytic mechanism of sulfur alkylation enzymes has been investigated using spectroscopy and model chemistry, and there are competing models of how the reaction occurs.[17] The thiolate could either dissociate from the zinc prior to the nucleophilic reaction or remain coordinated to the metal. Additionally, the functional significance of the different zinc coordination spheres used to catalyze such similar reactions is not known. Further characterization of the zinc sites at various steps of the reaction pathway is necessary to understand the catalytic mechanism of these metalloenzymes. Despite the presence of 10 crystal structures for FTase, there are many questions that remain unresolved: is the coordinating aspartic acid residue monodentate or bidentate; what are the zinc ligand bond lengths (crystallographic values for nominally equivalent bonds vary by up to 0.5 Å); and does the thioether of the product complex remain bound to the zinc? EXAFS is a method that can be used to characterize the geometry and metal ligand distances to high precision.[18,19] Therefore we have undertaken EXAFS studies of FTase to answer these questions and to provide further insight into the FTase mechanism.

Materials and Methods

Kinetic Methods. All assays were performed at 25 °C. Kinetics curve fitting used the nonlinear least-squares optimization in the program KaleidaGraph (Synergy Software). [³H]FPP was purchased from Amersham Pharmacia Biotech (Piscataway, NJ), vacuum-dried, washed with 100% methanol, and resuspended in 20 mM Heppso, pH 7.8, and 0.5 mM 3-14 zwittergent for a final concentration of 20 μM. The peptides GCVLS and TKCVIM were synthesized and purified by HPLC at Bethyl Laboratories, Inc. (Montgomery, TX), and the dansylated GCVLS was prepared by the University of Michigan Peptide Core (Ann Arbor, MI). The concentration of peptide was determined by reaction of the cysteine thiol with 5,5′-dithiobis(2-nitrobenzoic acid) (DTNB), using an extinction coefficient of 14 150 M⁻¹ cm⁻¹ at 412 nm.[20] FTase concentration was determined by UV absorbance at 280 nm using an extinction coefficient of 150 000 M⁻¹ cm⁻¹.[21] FPT Inhibitor II was purchased from Calbiochem-Novabiochem Corporation (San Diego, CA).

Preparation of FTase. Recombinant rat FTase was overexpressed in *Escherichia coli* and purified as described previously with the modifications described below.[22] The cell lysate was loaded onto a DEAE-Sephacel column (Pharmacia, 30 mL bed volume) preequilibrated with HTZ buffer (50 mM HEPES pH 7.8, 1 mM TCEP, 10 μM ZnCl₂). Proteins were fractionated using a linear gradient from 0 to 0.5 M NaCl in HTZ buffer. FTase eluted at 0.3 M NaCl. The fractions were tested for FTase activity by combining 50 mM Heppso pH 7.8, 5 mM MgCl₂, 1 mM TCEP, 0.2 μM FPP (Sigma), and 10 μL of protein sample in one well of a 96-well plate (90 μL total volume). The reaction was initiated by the addition of 10 μL of 10 μM Dns-GCVLS, and the fluorescence of each well was measured by the Polarstar Galaxy fluorescence plate reader (BMG Lab Technologies, Durham, NC, λ_{ex} = 320 nm, λ_{em} = 520 nm). The fractions with FTase activity were pooled and dialyzed against HTZ buffer overnight. The proteins were then further fractionated using a HiLoad 16/10 Q Sepharose FPLC column using the same salt gradient. The active fractions were again pooled and concentrated, and KCl was added to the protein sample for a total salt concentration of 2 M. The protein was then immediately loaded onto a HiLoad 16/10 Phenyl Sepharose FPLC column and fractionated, using a 2 M KCl to 0 M KCl gradient. FTase elutes in two peaks: peak 1 at 1 M KCl and peak 2 at 0 M KCl. Substrate binding studies with Dns-GCVLS demonstrated that the FTase isolated in peak 1 has a contaminant bound at the active site (data not shown); so peak 2 was used in all studies. The FTase sample was determined by SDS-PAGE to be >90% pure.

4-(2-Pyridylazo)resorcinol (PAR) Assay. The PAR assay was modified from a procedure published previously.[23] The FTase sample was diluted to 5 μM in 20 mM Tris pH 7.5 and 55 mM NaCl. Then 4-(hydroxymercuri)benzoic acid (0.5 mM) was incubated with the protein for 15 min to react with the protein cysteine thiols. PAR (0.1 mM) was added, and the absorbance of the Zn−PAR complex was measured at 500 nm. The concentration of zinc was determined using an extinction coefficient of 66 000 M⁻¹ cm⁻¹.

Pre-steady State Kinetics. Pre-steady state kinetic analysis was used to measure the pre-steady state burst amplitude in order to determine whether product was bound to the enzyme. A KinTek rapid quench apparatus was used to rapidly mix enzyme and substrate (KinTek Corporation, Austin, TX). The 30 μL reactions containing 0.1 μM FTase, 0.5 μM ³H-FPP, and 25 μM GCVLS were quenched with 80% 2-propanol and 20% acetic acid at varying times (0.01 to 10 s), then dried under vacuum and resuspended in 50% 2-propanol, as described previously.[24] The product was separated from substrate in these reactions by thin-layer chromatography on polyester-backed silica gel plates with an 8:1:1 (v/v/v) 2-propanol/NH₄OH/H₂O mobile phase. The product migrates in this mobile phase, but the FPP substrate does not; so the plates were cut accordingly and the radioactivity was quantified by scintillation counting. The counts per minute (CPM) of the product band were divided by the total CPM for each time point to calculate percent product formed, then multiplied by the initial FPP concentration to give the product concentration. Equation 1 was fit to the data, where P_t represents product formed at time t, E_0 is the initial enzyme concentration, k_1 is the rate constant of the burst phase, and k_2 is the rate constant of the linear phase.[25]

$$P_t = E_0 (1 - e^{k_1 t}) + E_0 k_2 t + C \qquad (1)$$

Active Site Titration. The concentration of FTase with zinc bound in the active site was determined by measuring the affinity of FTase+I2

(12) Zhang, F. L.; Moomaw, J. F.; Casey, P. J. *J. Biol. Chem.* **1994**, *269*, 23465−23470.
(13) Seabra, M. C.; Goldstein, J. L.; Sudhof, T. C.; Brown, M. S. *J. Biol. Chem.* **1992**, *267*, 14497−14503.
(14) Millian, N. S.; Garrow, T. A. *Arch. Biochem. Biophys.* **1998**, *356*, 93−98.
(15) Lin, Y. X.; Dotsch, V.; Wintner, T.; Peariso, K.; Myers, L. C.; Penner-Hahn, J. E.; Verdine, G. L.; Wagner, G. *Biochemistry* **2001**, *40*, 4261−4271.
(16) Gencic, S.; LeClerc, G. M.; Gorlatova, N.; Peariso, K.; Penner-Hahn, J. E.; Grahame, D. A. *Biochemistry* **2001**, *40*, 13068−13078.
(17) Parkin, G. *Chem. Commun.* **2000**, 1971−1985.
(18) Teo, B. K. *EXAFS: Basic Principles and Data Analysis*; Springer-Verlag: New York, 1986.
(19) Penner-Hahn, J. E. *Coord. Chem. Rev.* **1999**, *192*, 1101−1123.
(20) Riddles, P. W.; Blakeley, R. L.; Zerner, B. *Anal. Biochem.* **1979**, *94*, 75−81.
(21) Wu, Z.; Demma, M.; Strickland, C. L.; Syto, R.; Le, H. V.; Windsor, W. T.; Weber, P. C. *Protein Eng.* **1999**, *12*, 341−348.

(22) Zimmerman, K. K.; Scholten, J. D.; Huang, C. C.; Fierke, C. A.; Hupe, D. J. *Protein Expr. Purif.* **1998**, *14*, 395−402.
(23) Zamble, D. B.; McClure, C. P.; Penner-Hahn, J. E.; Walsh, C. T. *Biochemistry* **2000**, *39*, 16190−16199.
(24) Saderholm, M. J.; Hightower, K. E.; Fierke, C. A. *Biochemistry* **2000**, *39*, 12398−12405.
(25) Fierke, C. A.; Hammes, G. G. In *Enzyme Kinetics and Mechanism, Pt D*; Academic Press Inc.: San Diego, 1995; *Methods in Enzymology*, Vol. 249, pp 3−37.

for Dansyl-GCVLS.[10] The peptide binds at least 10-fold more tightly to the zinc-bound enzyme than the apo-enzyme. The binding of the peptide to the enzyme was observed by FRET (fluorescence resonance energy transfer) between the tryptophan residues of FTase (excitation at 280 nm) and the bound dansyl group (emission at 496 nm). The sample cuvettes contained 50 mM Heppso pH 7.8, 1 mM TCEP, 5 mM MgCl$_2$, 10 μM I2, and 500 nM FTase and were incubated for 15 min, allowing for formation of the FTase+I2 complex. The stoichiometric titration of FTase+I2 by Dns-GCVLS (0−1500 nM) was performed with a 2 min stirred incubation and a 1 min unstirred incubation prior to each measurement. Lines were fit separately to the first 10% of the binding titration and to the points > 500 nM, with the abscissa of the intersection point of the two lines representing the concentration of Zn-bound FTase in the sample.

EXAFS Sample Preparation. The active site zinc and other metals were removed from the FTase samples by dialysis of the protein against HT buffer (50 mM Hepes pH 7.8, 1 mM TCEP) with 5 mM EDTA for 24 h, followed by three changes against 500 mL of HT buffer with 25 g of Chelex (BioRad). The apo-protein was concentrated to about 60 μM and incubated overnight with 0.9 equiv of ZnCl$_2$ at 4 °C to reconstitute the Zn-bound protein. The protein was washed three times with 15 mL of 33 mM Bes pH 7.0 and 2.7 mM TCEP using spin filtration (Millipore Ultrafree, 10000 MWCO) to exchange buffer in the sample and eliminate any excess zinc and then concentrated to 200 μM. The zinc content of the protein was checked using the 4-(2-pyridylazo)resorcinol (PAR) assay described above.[26,27] The FTase was divided into four aliquots to make the samples E (FTase alone), E + I2 (binary complex), E + I2 + TKCVIM (ternary complex), and E + farnesylated TKCVIM (product complex). One aliquot of FTase was incubated with 0.9 equiv of FTase inhibitor I2 for 1 h on ice to make E + I2. The E + I2 + TKCVIM sample was prepared by incubating FTase with I2 as described above, then adding TKCVIM (0.9 equiv) and incubating on ice for 1 h. The E + farnesylated TKCVIM sample was prepared as described for the E + I2 + TKCVIM sample, but FPP was used in place of I2. All four samples were then concentrated to >500 μM, and glycerol was added to 25% v/v (60 μL total volume). The final buffer concentration after glycerol addition was 25 mM Bes pH 7.0, 2 mM TCEP, and the protein concentration ranged from 400 to 600 μM. The final zinc content was determined by inductively coupled plasma-mass spectrometry (ICP-MS) at the University of Michigan Department of Geological Sciences. The FTase + product sample was examined by matrix-assisted laser desorption/ionization mass spectrometry (MALDI-MS) at the University of Michigan Protein Structure Facility. The samples were loaded into Lucite cuvettes (~50 μL) with Kapton windows and frozen rapidly in liquid nitrogen. For the ternary complex and the product complex, independent duplicate samples were prepared. These gave identical fit results (see below).

XAS Measurements and Data Analysis. X-ray absorption spectra were measured at Stanford Synchrotron Radiation Laboratory (SSRL) on beam line 9-3 using a Si[220] double-crystal monochromator with a Rh-coated mirror upstream of the monochromator for harmonic rejection. The storage ring operated under normal conditions (3.0 GeV, 65−95 mA). Incident intensity was measured with an N$_2$-filled ion chamber. Energies were calibrated using the absorption spectrum of a zinc foil that was collected concurrently, with the first inflection point of the zinc foil spectrum defined as 9659 eV. Sample temperature was held at approximately 10 K using an Oxford liquid helium flow cryostat. X-ray absorption spectra were collected using a 30-element Ge solid-state detector. The total integrated count rates were held below 100 kHz/channel to avoid saturation, giving an average Zn Kα fluorescence count rate of 8 kHz. Each scan had 10 eV increments in the pre-edge region (9343−9643 eV), 0.35 eV increments in the edge region (9643−9690 eV), and 0.05 Å^{-1} increments in the EXAFS region. Integration

times were 1 s with pre-edge and edge regions and 1−10 s in the EXAFS region (k^3 weighted time through $k = 13$ Å^{-1} and constant at 10 s from $k = 13−19$ Å^{-1}) for a total scan time of ~45 min. Each detector channel of every scan (7 scans per sample) was checked for glitches, and the good channels (~28) were averaged for each sample to yield the final spectrum.

The XANES data were normalized to tabulated X-ray absorption cross sections using an error function plus a third-order polynomial to model the background over both the pre- and post-edge regions simultaneously.[28] EXAFS background correction was performed using AutoBK.[29] The data were then converted to k-space using $k = \sqrt{2m_e(E-E_0)/\hbar^2}$ where E_0 is 9664 eV. Fourier transforms were calculated using k^3 weighted data over a range of $k = 2−15.5$ Å^{-1} for all samples. Data analysis was performed using the GIFEFFIT program in R space from 0.7 to 3.0 Å.[30] The resulting filtered EXAFS data were fit to eq 2 using a nonlinear, least-squares algorithm.

$$\chi(k) = \sum_i \frac{N_i S_i A_i(k)}{kR_i^2} \exp(-2k^2\sigma_i^2) \sin(2kR_i + \phi_i(k)) \qquad (2)$$

In eq 2, N_s is the number of scatterers at a distance R_i, $A_i(k)$ is the effective backscattering amplitude, σ^2_i is the root-mean-square variation in R_i, $\phi_i(k)$ is the phase shift experienced by the photoelectron wave in passing through the potentials of the absorbing and backscattering atoms, and S_i is a scale factor (set to 0.9 for all samples[31]). The sum is taken over all scattering interactions. FEFF version 7.01[32] was used to generate phase and amplitude functions for Zn−S and Zn−N absorber−scatterer pairs, and Zn−S and Zn−N coordination numbers were varied as described previously.[31]

Results

Four different forms of FTase were measured in order to investigate the structure of the zinc site during the catalytic cycle. The samples follow the course of the FTase reaction as the enzyme first binds FPP, then binds the CaaX peptide substrate, and finally forms the enzyme product complex. To trap a ternary complex, the FPP analogue I2 was used with the TKCVIM peptide substrate; therefore, for comparison an FTase + I2 complex was used to model the FTase + FPP binary state. The product complex is an authentic (FPP + TKCVIM + FTase) E·P complex. To obtain successful FTase XAS samples, the zinc:enzyme ratio had to be monitored carefully to prevent extraneous zinc binding. The PAR assays in the course of sample preparation indicated that all of the XAS samples contained substoichiometric zinc, and ICP-MS analysis confirmed that in the final sample preparations the zinc:FTase stoichiometry was ≤1. The active site titration of the enzyme by Dns-GCVLS demonstrated that the zinc present in the sample was bound to the active site of FTase.

To confirm that the product complex contained bound product, pre-steady state kinetics and MALDI-MS were used to characterize these samples. Kinetic studies of the E, E + I2, and E + product samples show that the inhibitor and product ligands remain bound to the FTase active site after sample preparation. In the FTase kinetic mechanism, shown in Scheme

(26) McCall, K. A.; Fierke, C. A. *Anal. Biochem.* **2000**, *284*, 307−315.
(27) Hunt, J. B.; Neece, S. H.; Schachman, H. K.; Ginsburg, A. *J. Biol. Chem.* **1984**, *259*, 4793−4803.

(28) Waldo, G. S. Ph.D. Thesis, University of Michigan, Ann Arbor, 1991
(29) Newville, M.; Livins, P.; Yacoby, Y.; Stern, E. A.; Rehr, J. J. *Phys. Rev. B* **1993**, *47*, 14126−14131.
(30) Newville, M. *J. Synchr. Rad.* **2001**, *8*, 322−324.
(31) Clark-Baldwin, K.; Tierney, D. L.; Govindaswamy, N.; Gruff, E. S.; Kim, C.; Berg, J.; Koch, S. A.; Penner-Hahn, J. E. *J. Am. Chem. Soc.* **1998**, *120*, 8401−8409.
(32) Zabinsky, S. I.; Rehr, J. J.; Ankudinov, A.; Albers, R. C.; Eller, M. J. *Phys. Rev. B* **1995**, *52*, 2995−3009.
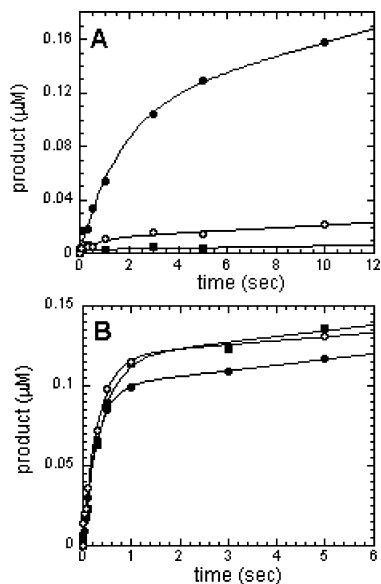
Figure 1. Pre-steady state kinetic studies of the protein samples. (A) Pre-steady state kinetics of XAS samples FTase (filled circles), FTase + I2 (filled squares), and FTase + product (open circles), as described in the text. The data were fit to eq 1 giving rate constants: FTase, $k_1 = 0.6 \pm 0.1$ s^{-1} and $k_2 = 0.005 \pm 0.001$ s^{-1}; FTase + I2, $k_2 = 0.003 \pm 0.004$ s^{-1}; FTase + product, $k_1 = 1.2 \pm 0.7$ s^{-1} and $k_2 = 0.0010 \pm 0.0004$ s^{-1}. The absence of a large burst in the FTase + I2 and FTase + product data indicates that ligands are bound in the active site. (B) Pre-steady state kinetics of XAS samples FTase (filled circles), FTase + I2 (filled squares), and FTase + product (open circles) when samples are preincubated with FPP prior to the reaction. For FTase, $k_1 = 3.6 \pm 0.2$ s^{-1} and $k_2 = 0.0036 \pm 0.006$ s^{-1}. For FTase + I2, $k_1 = 2.6 \pm 0.4$ s^{-1} and $k_2 = 0.004 \pm 0.02$ s^{-1}. For FTase + product, $k_1 = 3.1 \pm 0.5$ s^{-1} and $k_2 = 0.002 \pm 0.02$ s^{-1}. The recovery of the burst indicates these samples contain active enzyme. When the enzyme is not preincubated with FPP (panel A), the rate constant of the burst reflects the binding of FPP rather than product formation, with an expected k_{obs} given by [FPP]·$k_{on}^{FPP} = 1$ s^{-1}, close to the observed value of 0.6 ± 0.1 s^{-1}. All other values are consistent with previously published work under similar conditions.

Scheme 1. Kinetic Mechanism of FTase
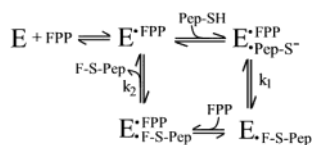
1, product release is the rate-limiting step ($k_1 > k_2$),[4] so that when the reaction is monitored at a short time scale in the presence of free enzyme, saturating FPP and GCVLS, a burst phase is observed followed by a linear phase. The burst phase mainly reflects the rate constant of product formation (k_1), since the free enzyme does not have to undergo the slow step of product release in the first turnover. The linear phase is indicative of the slower rate constant of product release (k_2) as the enzyme reaches a steady state. If there is a slowly dissociating ligand bound to the active site, however, the burst phase disappears, since the enzyme has to release inhibitor or product before binding substrate to begin catalysis. In the XAS samples (Figure 1A), the burst is present in the sample containing FTase alone, but disappears for the E + I2 and E + product complexes, indicating that in these samples the inhibitor and product, respectively, are still associated with the enzyme active site. To check the catalytic activity of the enzyme in these samples, this experiment was repeated under the same conditions, but the samples were preincubated with FPP prior to the
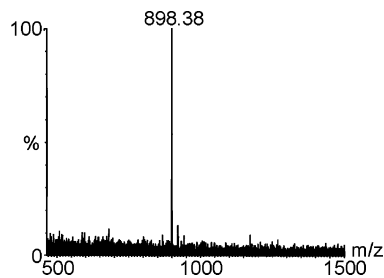

Figure 2. MALDI-MS spectrum of the FTase + product sample. The calculated mass of farnesylated TKCVIM is 898.27 g/mol.
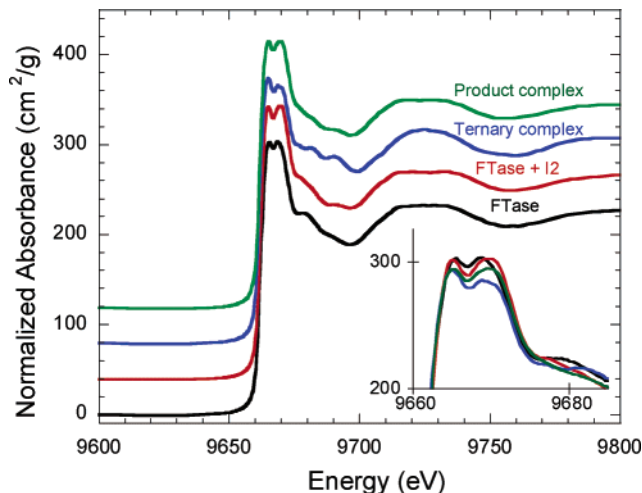

Figure 3. Normalized XANES for all protein samples. The inset contains an overlay of the normalized XANES, where FTase is black, FTase + I2 is red, FTase + ternary complex is blue, and FTase + product complex is green.

reaction. The FPP substrate binds tightly ($K_d = 6$ nM)[9] and can compete with the inhibitor and product for the active site. Under these conditions a burst of product reappears (Figure 1B), demonstrating that all of the enzyme samples can catalyze this reaction. Therefore, the loss of the burst phase is caused by the binding of I2 or product to the enzyme. Finally, MALDI-MS of the E + product sample demonstrates that the ligand bound to the enzyme has a molecular weight of 898.38 g/mol, consistent with the calculated molecular weight for farnesylated TKCVIM of 898.27 g/mol (Figure 2). These experiments demonstrate that the product samples contain authentic farnesylated TKCVIM product and that the product is bound to FTase.

The normalized XANES spectra for all four samples are nearly identical (see Figure 3) with two main peaks in the absorption edge, at ca. 9665 and 9670 eV. However, upon closer inspection, the spectra can be divided into two groups. FTase, FTase + I2, and FTase + product all have equal intensity for the 9665 and 9670 eV peaks, while the FTase ternary complex has a noticeably weaker 9670 eV peak. Although XANES spectra are known to be sensitive to the geometric structure of the absorbing site, it has been difficult to use them as more than a "fingerprint" for judging structural similarity. The peak at 9665 eV tends to increase in amplitude for sites that have more sulfur ligands.[11] Although there can be substantial deviation from this generalization, the increase in intensity at 9665 eV for the ternary complex thus suggests the presence of additional sulfur scatterers, while the similarity of the spectra for FTase, FTase + I2, and FTase + product suggests that there
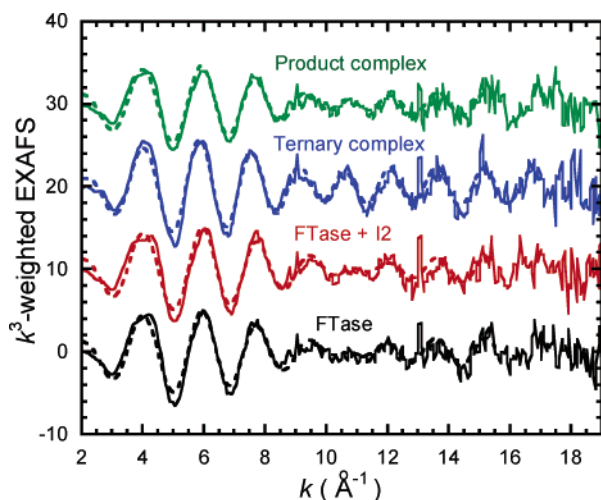
Figure 4. k^3-weighted EXAFS for all protein samples. The best fits (Table 1) are shown as dashed lines. All spectra are plotted on the same scale and offset vertically for clarity.
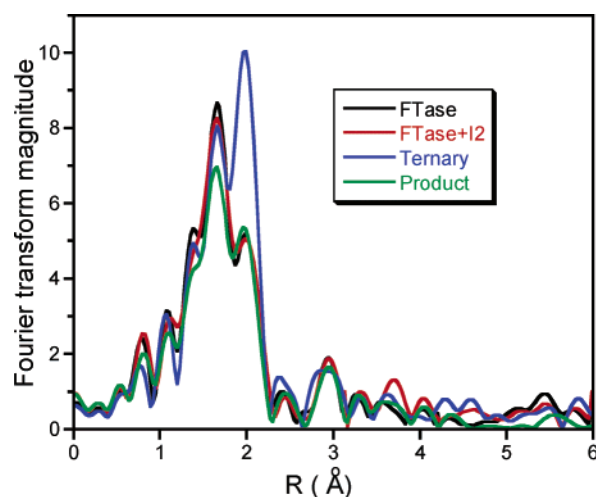
Figure 5. Fourier transform of all protein samples, where FTase is black, FTase + I2 is red, FTase + ternary complex is blue, and FTase + product complex is green. FT range was $2-15.5$ Å^{-1} for all samples.

is no significant change in either zinc ligation or zinc geometry when I2 or product binds.

As with the edges, the EXAFS spectra (Figure 4) for all four samples are quite similar, with the only significant difference being the amplitude of the oscillation at $k = 10-12$ Å^{-1} for the ternary complex. This difference arises from the addition of a second heavy scatterer, as shown clearly by the Fourier transform of the EXAFS data, Figure 5. All four Fourier transforms show evidence for two shells of nearest neighbor ligands, with the peaks at $R + \alpha \approx 1.7$ and 2.0 Å assigned to $Zn-(N/O)$ and $Zn-S$ scattering, respectively. In earlier studies of zinc alkyl transfer enzymes, the $Zn-(N/O)$ and $Zn-S$ contributions did not give rise to resolvable peaks in the Fourier transform.[16,33,34] Resolvable peaks are observed for FTase for two reasons: The number of sulfur scatterers, which dominate the EXAFS, is smaller. This makes the $Zn-N$ contribution more readily detectable. In addition, it was possible to collect the

(33) Gonzalez, J. C.; Peariso, K.; Penner-Hahn, J. E.; Matthews, R. G. *Biochemistry* **1996**, *35*, 12228−12234.
(34) Peariso, K.; Goulding, C. W.; Huang, S.; Matthews, R. G.; Penner-Hahn, J. E. *J. Am. Chem. Soc.* **1998**, *120*, 8410−8416.

Table 1. EXAFS Fitting Results for FTase[a]

	N/O			S			
sample	CN[b]	R (Å)[c]	$\sigma^2 \times 10^3$ (Å^2)	CN[b]	R (Å)[c]	$\sigma^2 \times 10^3$ (Å^2)	F′ [d]
FTase	3.0	2.041	3.1	1.3	2.315	3.6	24.0
	3	2.044	3.0	**1**	2.314	2.3	22.3
FTase + I2	2.9	2.041	3.1	1.2	2.305	3.0	22.4
	3	2.043	3.1	**1**	2.305	2.2	19.9
ternary complex	2.2	2.043	3.0	2.2	2.329	3.2	14.2
	2	2.046	2.5	**2**	2.328	2.7	14.0
ternary complex duplicate	2.5	2.049	4.2	1.9	2.330	3.0	12.4
	2	2.048	2.4	**2**	2.328	2.8	9.7
product complex	2.9	2.051	4.5	1.0	2.318	2.0	8.4
	3	2.051	4.7	**1**	2.318	2.1	7.3
product complex duplicate	3.2	2.050	5.8	0.8	2.322	1.2	6.9
	3	2.047	5.3	**1**	2.322	1.9	6.1

[a] Parameters in boldface were fixed during refinement. [b] Coordination number. [c] Bond length. Estimated accuracy is 0.02 Å; experimental precision is ca. 0.004 Å.

present data to higher resolution. This again increases our ability to resolve the $Zn-S$ and $Zn-(N/O)$ components. The Fourier transforms support the suggestion, based on the XANES spectra, that there is an additional sulfur ligand in the ternary complex, but that the other three complexes all have similar ligation. This is confirmed by quantitative curve fitting analysis (Table 1). FTase, FTase + I2, and FTase + product are all best fit using a single $Zn-S$ interaction and three $Zn-(N/O)$ scatterers. On the basis of crystallographic studies, the three low-Z scatterers must represent one histidine nitrogen, one aspartate oxygen, and either a water molecule or a second aspartate oxygen. The fits for the ternary complex are, as expected from Figure 5, quite different. These data could only be fit by including a shell of two sulfur atoms with a corresponding decrease in the number of $Zn-(N/O)$ interactions.

Although the product complex is very similar to the FTase and FTase + I2 complex, it does not give identical fit results. The bond lengths are identical within the estimated precision of 0.004 Å, but there is a small increase in the $Zn-(N/O)$ Debye−Waller factor. Debye−Waller factors, σ^2, which are a measure of the disorder in the absorber (Zn)−scatterer (ligand) distance, are notoriously difficult to define by EXAFS. However, the similarity of the value for the FTase and the FTase + I2 complex suggests a precision of 0.2 Å^2 for the present data. In this context, the increase in the $Zn-(N/O)$ but not the $Zn-S$ Debye−Waller factor for the product complex may be significant.

Discussion

A total of 10 crystal structures have been reported for FTase (see Table 2), all at a resolution of 2.0 Å resolution or worse. Given this level of resolution, the uncertainty in bond length is expected to be 0.3 Å or more.[35] Consistent with this expectation, quite different zinc−ligand distances are found for the two different FTase + FPP structures, the five different FTase ternary complexes, and the two different FTase product complexes. One of the interesting aspects of Table 2 is that the reported Zn−ligand distances are in general substantially longer than the Zn−ligand distances that are typically found in small molecules.[36] This has been observed for metalloproteins in

(35) Cruickshank, D. W. J. *Acta Crystallogr. Sect. D-Biol. Crystallogr.* **1999**, *55*, 583−601.

Table 2. Summary of FTase Crystal Structures

crystal structure[a]	resolution (Å)	pH	Zn–O (H₂O)	Zn–S (Pep)	Zn–S (Cys299)	Zn–O (Asp297)	Zn–O (Asp297)	Zn–N (His362)	Zn–N/O av	Zn–S av
1FT1 FTase alone	2.25	7.0	2.74		2.22	2.00	2.56	2.48	2.45	2.22
1FPP FTase + FPP	2.75	4.4	3.22		2.27	1.99	2.03	2.10	2.34	2.27
1FT2 FTase + FPP	3.4	7.0	NA		2.42	2.38	3.05	2.64	NA	2.42
1QBQ FTase ternary	2.4	5.7		2.48	2.21	1.90	2.45	2.24	2.20	2.35
1D8D FTase ternary	2.0	5.7		2.40	2.26	1.99	2.61	2.18	2.26	2.33
1JCS FTase ternary	2.2	5.7		2.35	2.21	2.08	2.55	2.17	2.27	2.28
1JCR FTase ternary	2.0	5.7		2.41	2.33	1.97	2.53	2.21	2.24	2.37
1JCQ FTase ternary	2.3	5.7		2.75	2.29	2.22	2.67	2.34	2.41	2.52
1KZP FTase product	2.1	5.7		2.66	2.27	2.06	2.42	2.18	2.22	2.47
1KZO FTase product + FPP	2.2	5.7			2.30	2.13	2.42	2.25	2.27	2.30

[a] 1FT1 (FTase alone)[2], 1FPP (FTase + FPP),[39] 1FT2 (FTase + FPP),[40] 1QBQ (FTase + αHP + TKCVIM),[6] 1D8D (FTase + I2 + KRas),[5] 1JCS (FTase + I2 + TKCVFM), 1JCR (FTase + FPP + CVFM), 1JCQ (FTase + FPP + L-739, 750),[7] 1KZP and 1KZO.[41] The four-character codes are the structure entries with the Protein Data Bank.

general, particularly for structures with poorer resolution.[36] The typical Zn−O and Zn−N distance for four-coordinate Zn coordinated to water, carboxylate, or histidine is 2.00 Å, while the typical Zn−S distance for thiolates is 2.29 Å.

The FTase EXAFS data resolve some of the uncertainties in the zinc site structure. In all four cases, the EXAFS-derived bond lengths are completely consistent with those expected for the equivalent small molecule crystal structures. Of particular interest are the nearly identical Zn−S and Zn−(N/O) distances that are found for all four of the FTase samples. From small molecule studies, it is known that the average Zn−ligand distance typically expands by ∼0.1 Å on going from four- to five-coordinate.[37,38] The nearly identical EXAFS bond lengths for the different FTase samples suggest that there is no change in the coordination number of the zinc. The best fits to the EXAFS data are consistent with a four-coordinate Zn site in each form of the enzyme.

The crystal structures for FTase have been interpreted as having a five-coordinate zinc site with four low-Z ligands (histidine, a bidentate aspartic acid, and a water).[2] For most of the crystal structures there is a broad range of Zn−(N/O) distances (the spread in Zn−N and Zn−O distances within a single structure varies from 0.4 to 1.3 Å). EXAFS data cannot address the question of whether a distant ligand is coordinated (e.g., a water at 2.7 Å or a carboxylate oxygen at 3.0 Å) since such distant ligands would not be expected to contribute to the observed EXAFS. However, the EXAFS data do allow us to place some restriction on the distribution of nearest neighbor distances. On the basis of the small Debye−Waller factors that are found for all of the data, the spread in Zn−(N/O) nearest neighbor distances is not larger than 0.10 Å. We conclude that only three of the four possible low-Z ligands are in fact tightly coordinated to the zinc (i.e., within a distance of 2.0−2.2 Å). It is impossible to tell from EXAFS which of these ligands is at a longer EXAFS undetectable distance, although the most likely candidates are the water and the second oxygen of the carboxylate. Of these, the water either is not seen (in 1FT2) or is more distant from the zinc than the second carboxylate oxygen (in 1FT1 and 1FPP) in the FTase crystal structures. Therefore, we favor a model in which the three low-Z ligands that are seen by EXAFS for FTase and FTase + I2 are the histidine nitrogen and the two oxygen atoms from the carboxylate side

chain of the aspartate. Although the alternative of a monodentate carboxylate and a tightly coordinated water cannot be excluded by the EXAFS data, the presence of a coordinated water in FTase would be deleterious to the farnesylation reaction due to potential hydrolysis of the FPP substrate. Hydrolysis of FPP is *not* catalyzed by FTase, suggesting that the enzyme protects bound FPP from water.[9] It could be that Asp 297 was evolutionarily conserved to serve as a flexible monodentate/bidentate ligand to replace water in the zinc coordination sphere of FTase. Given the small EXAFS Debye−Waller factor, the three Zn−(O/N) distances must all be clustered near the average value of 2.04 Å, suggesting either a tightly bound water or, in the model that we favor, a nearly symmetric bidentate carboxylate.

The EXAFS data for the FTase ternary complex clearly shows coordination of a second sulfur ligand, consistent with the crystal structures showing ligation of the substrate thiolate to the zinc. In contrast to the crystal structures, which show a difference of between 0.1 and 0.5 Å for the two Zn−S distances, the EXAFS spectra for the ternary complex show no significant disorder in the Zn−S shell. The maximum spread in Zn−S distances that would be consistent with the Debye−Waller factor is ca. 0.10 Å. This is significant, since it has been proposed that in zinc enzymes that catalyze sulfur alkylation the bond between the zinc and the thiolate substrate should be lengthened by the enzyme to allow for maximum nucleophilic character on the thiolate.[42] The small spread in the zinc−ligand distances suggests that this is not the case in FTase. There is a very small (ca. 0.02 Å) increase in the average Zn−S distance on going from FTase + I2 to the ternary complex, which *might* reflect a slight elongation (perhaps as much as 0.04 Å) of the Zn−S(peptide) bond. If such an increase takes place, it would be much smaller than the increase suggested by crystallography, although it should be noted that it is possible that the Zn−S(peptide) bond could be lengthened in an active ternary complex (E + FPP + TKCVIM) or in the transition state. Since the zinc appears to remain four-coordinate in the ternary complex, one of the low-Z ligands must be displaced when the peptide substrate binds. Water would be a natural candidate to be displaced by the incoming thiolate. However, if the water is more distant, as suggested by the crystal structures, it may be

(36) Harding, M. M. *Acta Crystallogr. Sect. D-Biol. Crystallogr.* **2001**, *57*, 401−411.
(37) Thorp, H. H. *Inorg. Chem.* **1992**, *31*, 1585−1588.
(38) Liu, W. T.; Thorp, H. H. *Inorg. Chem.* **1993**, *32*, 4102−4105.
(39) Dunten, P.; Kammlott, U.; Crowther, R.; Weber, D.; Palermo, R.; Birktoft, J. *Biochemistry* **1998**, *37*, 7907−7912.
(40) Long, S. B.; Casey, P. J.; Beese, L. S. *Biochemistry* **1998**, *37*, 9612−9618.
(41) Long, S. B.; Casey, P. J.; Beese, L. S. *Nature* **2002**, *419*, 645−650.
(42) Sun, L. J.; Yim, C. K.; Verdine, G. L. *Biochemistry* **2001**, *40*, 11596−11603.

instead that the carboxylate is converted from bidentate to monodentate when the peptide binds.

The most surprising structure is the FTase product complex, where both the XANES and the EXAFS data demonstrate a high degree of similarity to the FTase and FTase + I2 samples. Although the low-Z shell has a Debye–Waller factor that is slightly larger than in the other samples, the observed σ^2 is still well within the range seen for model compounds, suggesting that the apparent coordination number of three O/N ligands is correct. If a site with only two low-Z ligands was fit with three O/N ligands, the apparent Debye–Waller factor would be much larger. The presence of three low-Z ligands requires that one of the nearby ligands, possibly the second carboxylate oxygen, has come back into the Zn ligation sphere.

As with FTase and FTase + I2, the product complex is well modeled using only a single sulfur shell. Attempts to fit the data using a shell of two sulfur ligands give an unrealistically large Debye–Waller factor. Despite the structural similarity between resting FTase and the product complex, the product is clearly bound to the protein in the product complex, as demonstrated by the pre-steady state kinetics and the MALDI-MS results.

Taken together, these results suggest that the product must interact with FTase primarily through side chain interactions and not through a strong Zn–S bond. This is not in itself surprising, since it is known that thioethers are typically not bound in zinc inorganic complexes unless special precautions, for example macrocyclic ligands or noncoordinating solvents, are taken to promote coordination (see Table S1 for representative Zn–S(thioether) distances.[43]

However, two prior studies have concluded that the FTase thioether product *is* coordinated to the active site zinc, in apparent contradiction of the present results. The first study used UV–vis spectroscopy to characterize cobalt-substituted FTase bound to farnesylated peptide. Two distinctive shoulders were seen in the LMCT region (320 to 370 nm) with an intensity ($\epsilon = 1600\ M^{-1}\ cm^{-1}$) intermediate between that of resting FTase (one thiolate ligand, $\epsilon = 1030\ M^{-1}\ cm^{-1}$) and that of the ternary complex (two thiolate ligands, $\epsilon = 1900\ M^{-1} cm^{-1}$).[1] The intensity of the charge-transfer transition for the product complex would be consistent with mixed Co-thiolate + Co-thioether ligation,[44] thus suggesting that the thioether product remains coordinated to the Co (and thus presumably to the Zn). However, other factors, including thiolate-Co geometry, can affect the observed charge-transfer intensity, thus potentially complicating interpretation of the UV–visible spectra.

More recently, an X-ray crystallographic study of FTase bound to farnesylated peptide (FTase + product) and FTase bound to farnesylated peptide and a FPP substrate molecule (FTase + product + FPP) has also suggested that the thioether remains coordinated.[41] These structures revealed two possible conformations of the thioether product. In the FTase + product + FPP structure, the FPP displaces the farnesyl group of the product out of the active site and into a hydrophobic groove on the outside of the protein. The peptide moiety of the product remains in the active site, but adopts a turn so that the thioether is no longer coordinated to the zinc. A structure such as this

would be consistent with the absence of detectable Zn-thioether EXAFS. However, the EXAFS samples contained substoichiometric concentrations of the FPP and TKCVIM substrates, and therefore it is unlikely that an FTase + product + FPP complex would have been formed.

The other thioether complex, for FTase + product, shows the product in the active site, with the thioether sulfur remaining close to the zinc. However, the distance from the Zn to the thioether sulfur, 2.7 Å, is quite long. This is ca. 0.3 Å longer than the average Zn–S$_{thioether}$ distance in Zn model compounds (see Table S1).[43,45,46] Given the modest crystallographic resolution (2.1 Å), it is possible that the crystallographic data overestimate the true Zn–thioether distance, perhaps by as much as 0.3 Å. However, a short (ca. 2.4 Å) Zn–S$_{thioether}$ distance should be detectable by EXAFS. This was certainly the case in EXAFS studies of the methylated Ada protein, where methylation of a Zn-bound thiolate resulted in a noticeable elongation of the Zn–S$_{thioether}$ distance together with a concomitant decrease in the remaining Zn–ligand distances.[15] Neither the long Zn–S distance nor the decrease in the remaining Zn–ligand distances is observed in the EXAFS data for FTase, suggesting that the FTase product complex does not contain a short (2.4 Å or less) Zn–S$_{thioether}$ distance. An alternative possibility is that the true Zn–S$_{thioether}$ distance in the product complex is 2.7–3.0 Å. A distance this long would result in an extremely weak Zn–S$_{thioether}$ interaction, which would be unlikely to be detectable by EXAFS.[47,48] At such a long distance, the thioether would make a negligible contribution to the bonding at the Zn site.[49] The strength of the Zn–S$_{thioether}$ interaction will be explored in future studies by replacing the thiolate sulfur in the substrate peptide with selenium, thus allowing more thorough examination of the zinc–selenoether interaction.

Conclusions

The zinc site in FTase is coordinated by a histidine, a cysteine, and most likely a bidentate aspartate in its resting state. A fourth low-Z ligand, for example from the water that is seen in many crystal structures, does not make a detectable contribution to the EXAFS and is thus presumably at a longer distance from the zinc. The binding of the FPP analogue I2 does not cause any significant change in the zinc site geometry or ligation. Upon peptide binding, one low-Z ligand, most likely one of the aspartate oxygens, is displaced by the peptide cysteine thiol. After transfer of the C1 of FPP to the peptide thiolate to form the thioether product, the zinc returns to ZnS(N/O)$_3$ ligation, indicating that the Zn–S$_{thioether}$ interaction is extremely weak, with the thioether having been effectively displaced by a low-Z ligand, most likely the second oxygen from the carboxylate. Structural changes such as these, with alternation of the carboxylate from monodentate to bidentate, would provide an effective mechanism to increase the nucleophilicity of the peptide thiolate during the farnesyl transfer reaction. Conversion of the carboxylate toward bidentate ligation in the transition

(43) Grapperhaus, C. A.; Tuntulani, T.; Reibenspies, J. H.; Darensbourg, M. Y. *Inorg. Chem.* **1998**, *37*, 4052–4058.
(44) Sellmann, D.; Neuner, H. P.; Knoch, F. *Inorg. Chim. Acta* **1991**, *190*, 61–69.

(45) Hammes, B. S.; Carrano, C. J. *Inorg. Chem.* **2001**, *40*, 919–927.
(46) Chiou, S. J.; Innocent, J.; Riordan, C. G.; Lam, K. C.; Liable-Sands, L.; Rheingold, A. L. *Inorg. Chem.* **2000**, *39*, 4347–4353.
(47) Scott, R. A.; Hahn, J. E.; Doniach, S.; Freeman, H. C.; Hodgson, K. O. *J. Am. Chem. Soc.* **1982**, *104*, 5364–5369.
(48) Penner-Hahn, J. E.; Murata, M.; Hodgson, K. O.; Freeman, H. C. *Inorg. Chem.* **1989**, *28*, 1826–1832.
(49) Xiang, S. B.; Short, S. A.; Wolfenden, R.; Carter, C. W. *Biochemistry* **1996**, *35*, 1335–1341.

state could shift electron density onto the peptide cysteine, thus increasing the nucleophilicity of the zinc-thiolate and facilitating catalysis of farnesylation. This would be analogous to the "valence buffer" mechanism proposed for cytidine deaminase.[49]

Supporting Information Available: Table of Zn−S distances for tetrahedral Zn-thioether model complexes together with structurally related zinc thiolate models. This material is available free of charge via the Internet at http://pubs.acs.org.

JA035927O